Environmental Science and Pollution Research
https://doi.org/10.1007/s11356-024-34694-9

RESEARCH ARTICLE

Assessment of the mobility of potentially toxic trace elements (PTEs) and radionuclides released in soils stabilized with mixtures of bentonite-lime-phosphogypsum

Achraf Harrou[1] · Meriam El Ouahabi[2,3] · Nathalie Fagel[3] · Alejandro Barba-Lobo[4] · Silvia M. Pérez-Moreno[4] · Juan Pedro Bolívar Raya[4] · ElKhadir Gharibi[1]

Received: 4 June 2024 / Accepted: 8 August 2024

Abstract

Phosphogypsum (PG) is a solid by-product of the phosphate industry, rich in contaminants and produced in large quantities. Raw materials and stabilized specimens, consisting of bentonite-lime-PG mixtures, were characterized by mineralogical, microstructural, chemical, alpha-particle, and gamma-ray spectrometry analysis before hydration and after hardening. Compressive strength and leaching tests were performed on hardened specimens. The physicochemical parameters and chemical composition of leachates from raw materials and hardened specimens were determined. PG contains high concentrations of natural radionuclides, specially from U series. Uranium-238 activities are double in PG than the worldwide average for soil values. The mobility of PTEs from PG is Cd (2.43%), Zn (2.36%), Ni (2.07%), Cu (1.04%), Pb (0.25%), and As (0.21%). Cadmium is the cation most easily released by PG in water with a concentration 0.0316 mg kg^{-1}. When PG is added to bentonite-lime mixture, cadmium is no longer released. The radionuclide $^{238,234}U$ and ^{210}Po predominates in the leachates of PG. However, the activity of ^{210}Po becomes negligible in the leachates of bentonite-lime-PG mixtures. The addition of PG to bentonite-lime mixtures facilitates the trapping of trace elements (PTEs) and radionuclides, providing potential applications for PG as road embankments and fill coatings.

Keywords Natural radionuclides · Transfer factor · Leaching · Environmental contamination · Phosphogypsum

Introduction

Phosphate rocks in Morocco can contain high amounts of natural radionuclides, particularly those belonging to the ^{238}U series, rare earth elements (REEs) (Al Khaledi et al. 2019), and potentially toxic trace elements (PTEs) (Kechiched et al. 2020). During chemical attack, for the production of phosphoric acid or phosphate fertilizers, dangerous pollutants such as heavy metals and natural radionuclides can migrate into the phosphogypsum (PG) (Qamouche et al. 2020). Many studies shed light on the impact of PG in environment, especially with respect to the distribution of REEs (Cánovas et al. 2019; Mukaba et al. 2021), PTEs (e.g., As, Cd, Pb, Cu, Cr, Ni, Zn, Mn, Sb) (Pérez-Moreno et al. 2018; Ramanayaka et al. 2019), natural radionuclides (Moreno et al. 2023; Papaslioti et al. 2020; Pérez-Moreno et al. 2018, 2023), and anions (F^-, PO_4^{3-}, and SO_4^{2-}) (Pérez-Moreno et al. 2023). In Mediterranean costal area, several studies emphasized the potential environmental risks of the PG and its significant contribution to radioactive contamination of coastal waters (Bolıvar et al. 2002; El Zrelli et al. 2019; Pérez-López et al. 2011; Periáñez et al. 2013). The secular equilibrium of radionuclides belonging to the ^{238}U series is broken during the acid attack of the phosphate rock and 100% of ^{210}Pb, 90% of ^{226}Ra, 80% of ^{232}Th plus ^{230}Th, and 78% of ^{210}Po fractionate to PG (Mazzilli et al. 2000). The discharge of PG into the open sea from Morocco has caused the contamination by ^{238}U, ^{226}Ra, and ^{210}Po in the natural sand of the beach of the El Jadida province (Belahbib et al. 2021).

PG represents a worldwide environmental problem. In 2013, the annual worldwide production of PG was around 160 million tonnes. Forecasts by the International Atomic Energy Agency (IAEA 2013) indicate an increase that could reach 200 to 250 million tonnes within the next

Responsible Editor: Kitae Baek

Extended author information available on the last page of the article

Published online: 21 August 2024

decade or two. PG is often stored in large stacks or piles in dedicated storage areas (Hilton 2008). There are about 6 billion tonnes of PG stored in stacks worldwide (IAEA 2013). This accumulation of PG results in the release of hazardous substances, which can have a severe environmental impact, such as air, soil, river, or groundwater pollution (Silva et al. 2022). The nature of the soil at PG storage sites influences the release of contaminants. The stack of PG should be constructed above the ground level and on natural clayey soils, specifically on adsorbent clays such as smectite-rich clays, to prevent any infiltration (Bhawan and Nagar 2014). Another problem of PG stacks is the ^{222}Rn exhalation through the surface if it has not been restored with insulator materials from Rn (Dueñas et al. 2007).

Bentonite is a clay rich in natural colloidal expansive smectite, containing adsorption sites in the interlayer space, the external surface, and edges. It is an excellent sorbent for trace elements, making it highly effective for water pollutant treatment (Han et al. 2022). The high surface area and pore size of natural bentonite make it a good adsorbent for REEs from wastewaters (Mosai et al. 2019). The interlayer space retains cations, while the most REEs soluble species are anionic oxygen combined, especially in circum-neutral pH (Vriens et al. 2019). The addition of lime to bentonite can generate intraparticle porosity, enhancing the sorption of REEs (Gaona et al. 2012; Kechiched et al. 2020). To reduce the amount of PG released into the environment, several researchers have proposed solutions, such as the incorporation of PG into a bentonite-lime mixture to develop a new material for road embankments (Kumar et al. 2014; Mashifana et al. 2018). The uniaxial compressive strength of specimens prepared with different mass fractions of PG, bentonite, and lime increases with the increase in the addition of PG added to the bentonite-lime mixture (Oumnih et al. 2019). The addition of PG to the bentonite-lime mixture affects the mineralogy of bentonite allowing the formation of ettringite (Harrou et al. 2020). However, previous studies have not assessed the release of toxic elements and radionuclides present in PG-bentonite-lime mixtures into water. A study of the leaching of PG-bentonite-lime mixtures could shed light on the rate at which pollutants are released from these mixtures.

Considering the aforementioned issues, this study investigates the leaching of raw clay mortar specimens composed of bentonite, hydraulic lime, and variable quantities of PG. The study aims to assess the feasibility of establishing PG storage sites on clayey soils rich in bentonite stabilized with hydraulic lime. It seeks to examine the capacity to retain pollutants present in the PG within the solidifying clayey soil through pozzolanic reactions between bentonite and hydraulic lime. Additionally, this approach will provide insights into the potential utilization of PG as road embankments and fill materials.

Material and methods

Raw materials

The phosphogypsum (PG) used in this study is produced by the Office Cherifien of Phosphates (OCP) group in Jorf Lasfar in Morocco. The bentonite (B) comes from the Trebia deposit (northeast of Morocco), which is the largest Moroccan deposit with a high economic performance (Lamrani et al. 2021). It is originating from hydrothermal alteration of obsidian perlite glass inside the volcanoes themselves (Ddani et al. 2005). This bentonite is rich in smectite, a 2:1 type clay mineral whit structure composed of two tetrahedral sheets [SiO_4] and an octahedral sheet [$(Al,Mg)O_4(OH)_2$]. The Trebia bentonite is characterized by high cation exchange capacity (146.5 meq/100 g) and a large specific surface (693 $m^2\ g^{-1}$) (Ait Hmeid et al. 2021). The hydraulic lime (L) sample, obtained by traditional calcination of local limestone, was purchased at local market in Oujda (northeast Morocco) (Fig. 1). To obtain representative results, three samples of each raw material were collected and homogenized prior to analysis. Three replicates were obtained for various characterization and leaching tests.

The formulation of PG-B-L mixtures was carried out by substituting B with a variable amount of PG ranging from 2 to 32%. The added L content was kept constant at 8% by mass (Table 1). The chosen L content is based on the results of our previous work, which showed that the mechanical strength of the B-L mixture is maximized with 8% L (Harrou et al. 2020; Kumar et al. 2014; Oumnih et al. 2019). For each experimental condition, three samples were analyzed, and average values are given. A total of 36 specimens were prepared: 18 for the mechanical compression test and 18 for the leaching tests.

Leaching specimens

The raw materials (PG, B, L) were crushed and sieved through a 250-µm mesh size before use. The leaching tests were carried out according to the standards "Assessment of release of dangerous substances. Horizontal dynamic surface leaching tests" (CEN/TS 16637–2). Demineralized water is used for leaching tests on the specimen, as it can be considered as rainwater. Firstly, cubic test specimens of 4 cm in size were prepared using the mass fraction of the B-L-PG mixed materials outlined in Table 1. The solid/

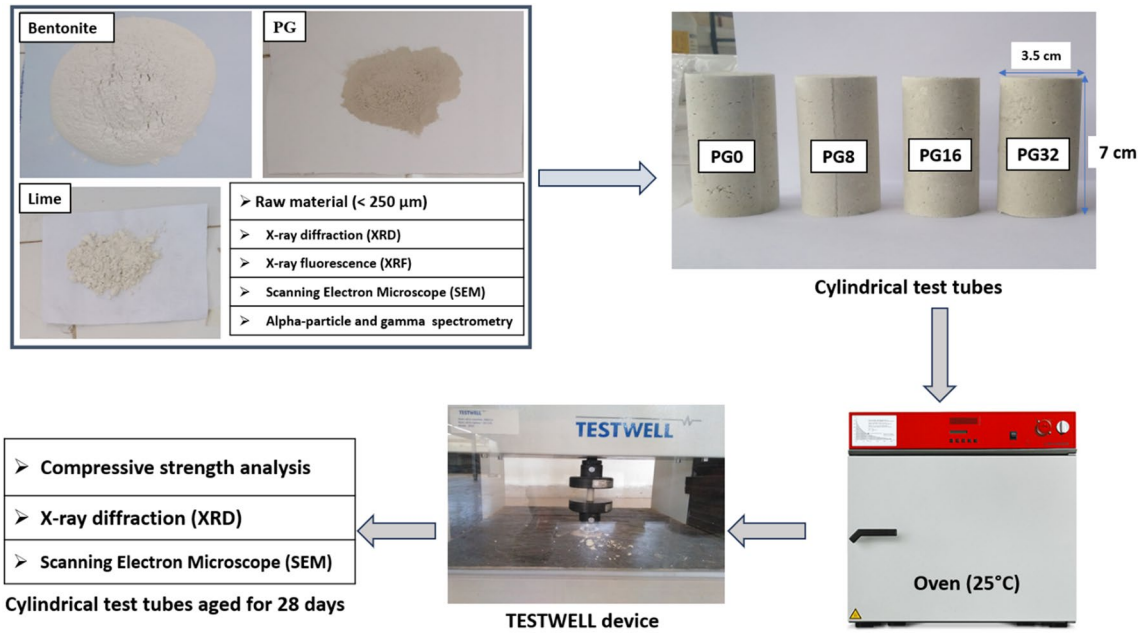

Fig. 1 Mortar specimens and schematic diagram of the compressive strength tests

Table 1 Formulation of specimens for leaching tests

Specimens	Mixtures: %PG + %B + %L
PG0	0%PG + 92%B + 8%L
PG8L0	8%PG + 92%B + 0%L
PG2	2%PG + 90%B + 8%L
PG8	8%PG + 84%B + 8%L
PG16	16%PG + 76%B + 8%L
PG32	32%PG + 60%B + 8%L

liquid ratio was 46% (Harrou et al. 2020). Subsequently, the specimens were covered with plastic film to prevent calcite formation and promote the formation of hydrated gels in the clay paste after 28 days of hydration at a room temperature of 20 °C. Hardened specimens, each weighing approximately 100g, were submerged in 1 L of demineralized water. Filtrations of 45 µm were conducted at intervals from 0.25 to 36 days to separate leachates from solids, with the system being replenished with fresh demineralized water after each filtration (Fig. 2). The release kinetics of chemical elements, including cations and anions, into the demineralized water, as well as variations in physicochemical parameters such as pH, EC, and redox potential, were monitored. Cation concentrations were determined by inductively coupled plasma mass spectrometry (ICP-MS), while anion concentrations were measured by ion chromatography (IC). Long-lived radionuclides (U isotopes, Th isotopes, Ra isotopes, and ^{210}Po) were measured by alpha particle spectrometry. The activity of ^{210}Pb was measured on the 46.5-keV gamma line by low-energy gamma spectrometry.

For raw materials, a similar process was followed, with specimens immersed for 24 h to achieve extreme ion leaching due to the low ionic strength of demineralized water.

The transfer factor (TF) was determined by calculating the ratio of trace element concentrations in leachates to those in the raw materials, as described by the following equation (Guido-Garcia et al. 2021) (Eq. 1):

$$TF(\%) = \frac{[X_L]}{[X_S]} * 100 \quad (1)$$

with:

(i) $[X_L]$: Concentration of the chemical element determined by ICP-MS in the leachate, in mg kg^{-1}.
(ii) $[X_S]$: Concentration of chemical element determined by ICP-AES in the solid phase prior to leaching, mg kg^{-1}.

The optimum concentrations, $A_{opt(S)}$ from the solid raw materials and $A_{opt(L)}$ from the concentrations of the raw materials, in the leachate are calculated by the Eqs. 2 and 3:

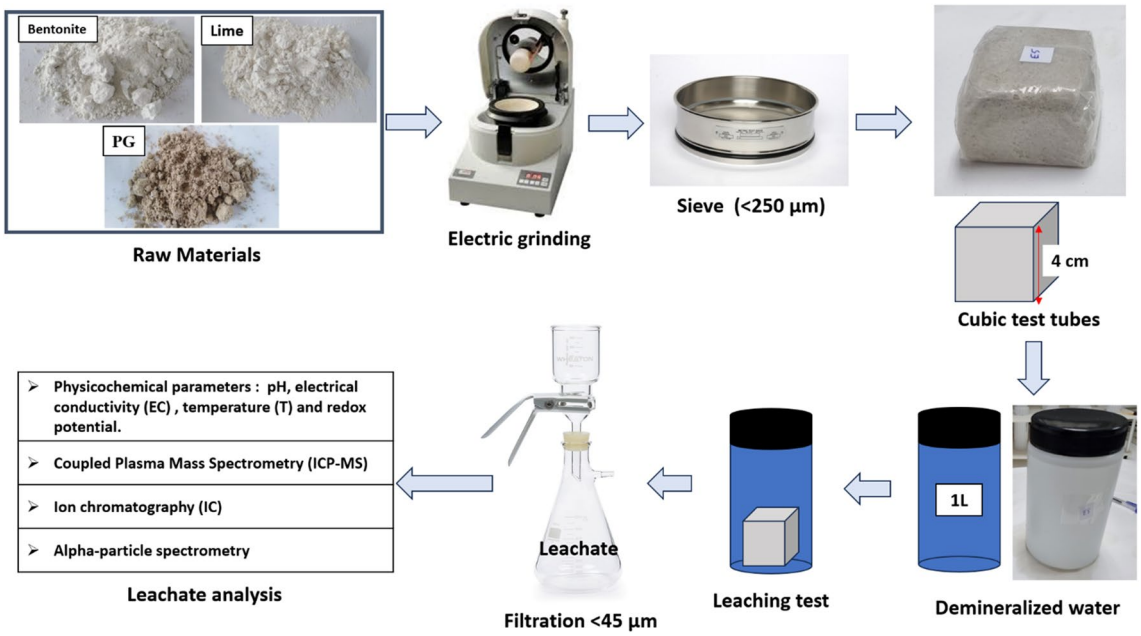

Fig. 2 Mortar specimens and schematic diagram of the leaching tests

$$A_{opt(S)}=X_B{*}A_{B(S)}+X_L{*}A_{L(S)}+X_{PG}{*}A_{PG(S)} \quad (2)$$

$$A_{opt(L)}=X_B{*}A_{B(L)}+X_L{*}A_{L(L)}+X_{PG}{*}A_{PG(L)} \quad (3)$$

with:

- $A_{B(S)}$, $A_{L(S)}$, and $A_{PG(S)}$: Concentrations of alpha-emitting radionuclides (Bq kg^{-1}) contained in B, L, and PG.
- $A_{B(L)}$, $A_{L(L)}$, and $A_{PG(L)}$: Concentrations of alpha-emitting radionuclides (Bq kg^{-1}) contained in the leachates of B, L, and PG, respectively, following a 24-h leaching period.
- X_B, X_L, and X_{PG}: Mass fraction of B, L, and PG in the specimens (Table 1)

The ratios R_L and R_S between the concentrations of alpha-emitting radionuclides measured in specimen leachates ($A_{exp(specimen)}$) and the optimum concentrations, $A_{opt(L)}$ and $A_{opt(S)}$, respectively, are calculated from Eqs. 4 and 5:

$$R_L=\frac{A_{exp(PG32)}}{A_{opt(L)}}*100 \quad (4)$$

$$R_S=\frac{A_{exp(PG32)}}{A_{opt(S)}}*100 \quad (5)$$

with:

$A_{exp(specimen)}$: Concentrations of alpha-emitting radionuclides (Bq kg^{-1}) contained in leachates of specimen after a leaching period of 16 days.

Analytical methods

Various techniques were employed to characterize and determine potentially toxic trace elements in both leachates from raw materials and cured specimens. All the equipment used is located in research centers and is systematically calibrated: All radiological and physicochemical analyses of PG and samples containing PG were carried out within 100 days of PG production at the Jorf Lasfar plant.

- X-ray diffraction (XRD) was carried out by a Shimadzu XRD 6100 diffractometer, equipped with a Cu X-ray tube, operating at 40 kV and 30 mA, in the interval [2–70°] 2θ. This analysis was performed in the Analytical Platform of Faculty of Sciences (Oujda).
- Scanning electron microscope (SEM) was used to determine the microstructure of the raw material and the cured specimens. The apparatus was an HIROX SH-5000P with high resolution, high vacuum, and SE and BSE detector (Oujda).
- The TESTWELL device was used for compressive strength analysis on cured specimens, with a speed of 1 mm/min (Oujda). We chose 28 days of hydration because this time gives mortars high compressive strength at room temperature.

- X-ray fluorescence (XRF) analysis was performed using Panalytical Sequential Spectrophotometer (ZETIUM Minerals model) in the Central Research Services of the University (Seville).
- Inductively coupled plasma atomic emission spectrometry (ICP-AES) was used for the analysis of chemical elements in the raw material performed by the Jobin Yvon Ultima 2 apparatus in Central Research Services of the University (Huelva)
- Inductively coupled plasma mass spectrometry (ICP-MS) was used for the analysis of cations concentration in leachate produced by the Agilent 7700 apparatus (Huelva).
- Ion chromatography (IC) analysis was performed by Metrohm 883 plus basic ion chromatograph (IC) equipped with Metrosep columns (Huelva).
- Physicochemical parameters, including pH, electrical conductivity (EC), and redox potential (Eh), were measured using a portable multiparametric probe (model Crison MM 40 +). The redox potential measured by the multiparametric probe is the oxidation–reduction potential (ORP). This value was corrected for temperature to obtain the standardized redox potential (Eh). The redox potential was calculated using the standard method proposed by Nordstrom and Wilde (1998). These measurements were conducted in the research group "Radiation Physics and Environment" (FRYMA-Huelva).
- Alpha-particle spectrometry was performed with passivated implanted planar Si (PIPS) detectors, EG & G ORTEC. The radiochemical procedure to isolate the U, Th, and Po isotopes was based on the methodology described by Pérez-Moreno et al. (2023) (FRYMA-Huelva). In leachate, measurements of alpha activity concentrations were carried out immediately after filtration.
- Gamma-ray spectrometry with a high purity germanium detector (HPGe model GCW3023) was employed. Gamma emitter measurements were carried out according to the procedure described by Barba-Lobo et al. (Barba-Lobo et al. 2021). Certified reference materials (CRM) from the IAEA, specifically RGU^{-1}, RGTh^{-1}, and RGK^{-1}, containing natural radionuclides from the ^{238}U, ^{232}Th, and ^{40}K series, were used to determine the experimental efficiencies (FRYMA-Huelva).

Results and discussion

Raw material characterization

Potentially toxic trace elements (PTEs)

The concentrations of PTEs in mg kg^{-1} for raw materials, namely B, L, and PG, were determined by ICP-AES analysis (Table S2 in Supplementary materials). Compared with the recommended trace element composition of the upper continental crust (Rudnick and Gao 2010), high concentrations of Be, Zn, Ga, As, Sr, Zr, Sn, Y, Cd, Ba, and Ce were observed in B. L shows increased concentrations of Co, Cu, Zn, As, Sr, Mo, Cd, and Pb, while PG shows high concentrations of Sr, Y, Mo, Cd, and U. The studied B is rich in Th (118.87 mg kg^{-1}). This value is higher than the average value of Th concentration found in soils, which typically varies from 2 to 12 mg kg^{-1} (Kabata-Pendias 2000). The concentration of Ba in the B is 2742.14 mg kg^{-1}. L and PG contain respectively 1037.11 mg kg^{-1} and 1166.64 mg kg^{-1} of Sr. Strontium, sharing similarities with calcium in its properties, is more mobile in soil than calcium, and its sorption into soil is linked to isomorphic replacement of calcium-containing minerals (Dubchak 2018; Ermakov et al. 2020). The uranium concentration in PG (12.31 mg kg^{-1}) is higher than that found in B (5.25 mg kg^{-1}) and L (1.76 mg kg^{-1}), and it exceeds the average value of 2.7 mg kg^{-1} identified in undisturbed soils. These concentrations fall within the range of soil concentrations, which typically are between 0.4 and 6 mg kg^{-1} expect for PG (Shacklette and Boerngen 1984).

The PTEs concentration results found in this study (Table 2) are within the range of concentrations reported in PGs originating from Morocco (Guerrero et al. 2019). Differences in trace element concentrations are observed when compared to other PGs from other countries (El Zrelli et al. 2018; Rutherford et al. 1994).

Alpha and gamma emitters

Table 3 shows the radionuclide activity concentrations of the raw material (B, L, and PG). The activity concentrations of the alpha emitters in B sample were similar to current worldwide average values (UNSCEAR 2008). The activity concentration of ^{210}Po is 18.4 ± 1.3 Bq kg^{-1} in B, which is close to that found in various soils 20–240 Bq kg^{-1} (Persson and Holm 2011). The ^{232}Th concentration obtained for L sample (182.4 ± 16 Bq kg^{-1}) is about four times higher than that found for an unpolluted soil (45 ± 4 Bq kg^{-1}) (UNSCEAR 2008). Thorium is commonly transported and redeposited by adsorption on clay-sized detrital grains (Bodin et al. 2011) and adsorbs preferentially on carbonates (Kretschmer 2010).

In general, PG contains significant concentrations of U-series radionuclides, with average activity concentrations around 650, 600, 400, and 100 Bq kg^{-1} for ^{226}Ra, ^{210}Po, ^{230}Th, and ^{238}U, respectively (Pérez-Moreno et al. 2018). The studied PG contains concentrations of ^{210}Po (699 ± 23 Bq kg^{-1}) and ^{230}Th (782.4 ± 53.9 Bq kg^{-1}) significantly higher than average concentrations. For ^{238}U, the concentration is 74.5 ± 3.2 Bq kg^{-1}, it is lower than the average concentration 100 Bq kg^{-1}, but it is double the worldwide average soil values (37 ± 4 Bq kg^{-1}) (UNSCEAR 2008). The activity concentration of ^{234}U is 75.7 ± 3.3 Bq kg^{-1} in PG, which is lower

Table 2 Comparison of potentially toxic trace element concentrations in PG with other studies

Elements (mg kg^{-1})	This study	Morocco		Tunisia	Florida	Idaho
		Guerrero et al. (2019)		El Zrelli et al. (2018)	Rutherford et al. (1994)	
As	3.25 ± 0.51	16 ± 7	0.5–83	1.0 ± 0.1	0.4	0.6
Cd	3.25 ± 0.09	1.8 ± 0.4	0.8–4.4	17.7 ± 1.8	< 0.2	10.7
Cr	35.75 ± 0.87	16 ± 3	8–36	13 ± 1.3	5	48
Cu	5.37 ± 0.88	32 ± 11	1.3–113	9.6 ± 1.4	3.4	11.4
Ni	3.84 ± 0.82	1.6 ± 0.6	0.05–6.1	4.1 ± 0.41	5	5
Pb	4.56 ± 0.03	36 ± 31	0.6–344	0.9 ± 0.09	10	13
Sb	< 0.1	2.8 ± 2.3	0.1–23.9	0.09 ± 0.01	10	13
Mn	13.01 ± 0.73	15 ± 2	4–20	< 5	-	-
Th	3.39 ± 0.01	0.9 ± 0.2	0.2–2.1	0.74 ± 0.07	1.5	-
U	12.31 ± 1.56	12 ± 2	2.8–28	1.6 ± 0.16	4.5	7.3
V	11.05 ± 0.42	6.3 ± 2.4	2–28	3 ± 0.3	6	20
Zn	12.23 ± 0.13	22 ± 8	2–98	137 ± 13.7	6.4	30.7
Y	106.34 ± 6.90	50 ± 4	30–78	53.2 ± 8.0	71	125

Table 3 Average activity concentration (Bq kg^{-1}) for radioelements contained in raw materials

Alpha activity	^{238}U	^{234}U	^{230}Th	^{234}U/^{238}U	^{232}Th	^{230}Th/^{232}Th	^{210}Po
B	21.4 ± 2.5	28.9 ± 2.0	6.21 ± 1.1	1.35 ± 0.11	7.21 ± 0.8	0.86 ± 0.13	18.4 ± 1.3
L	9.53 ± 1.1	9.96 ± 1.2	27.5 ± 5.1	1.04 ± 0.06	**182.4 ± 16**	0.15 ± 0.02	7.3 ± 0.6
PG	**74.5 ± 3.2**	75.7 ± 3.3	782.4 ± 53.9	1.02 ± 0.05	11.5 ± 3.6	**67 ± 10**	699 ± 3
W1	37 ± 4			1.02 ± 0.03	45 ± 4	**57 ± 17**	
W2	100	-	400		-		600
Gamma emission	^{226}Ra	^{228}Ra	^{234}Th	^{226}Ra/^{228}Ra	^{228}Th	^{40} K	^{210}Pb
Gamma energies (keV)	351.9	911.2	63.3		238.6	1460.8	46.5
B	24.7 ± 1.3	219 ± 9.1	45.6 ± 4	0.11 ± 0.01	217.9 ± 9,2	285.1 ± 14	26.9 ± 3
L	11.1 ± 0.9	6.87 ± 2.8	10.2 3	1.62 ± 0.14	8.88 ± 1.6	87.7 ± 9	13.4 ± 4
PG	**815 ± 33**	14.1 ± 3.8	88.1 ± 9	58 ± 7	13.4 ± 1.7	29.5 ± 12	805.8 ± 35
W1	33 ± 3					400 ± 24	
W2	650		-		-	-	-

W1 worldwide in raw materials (UNSCEAR 2008), *W2* average activity concentration in PG (Pérez-Moreno et al. 2018)

than the concentration found in PGs produced in Huelva obtained from phosphates coming from Morocco (Bolıvar et al. 2002; Dueñas et al. 2010) and Morocco (Azouazi et al. 2001). The concentration of ^{232}Th in PG is relatively low (11.5 ± 3.6 Bq kg^{-1}), consistent with values reported in PG from Moroccan phosphate (Bolıvar et al. 2002; Dueñas et al. 2010). The isotopic fractionation of radionuclide shows that the activity ratio of ^{230}Th/^{232}Th in B is close to 1. This aligns with the average ratio observed in detrital river particles and, consequently, in nearshore sediment (Sam et al. 2000). For L, the ^{230}Th/^{232}Th activity ratio is less than 1, indicating detrital contributions (Ludwig et al. 2011). For PG, the ratio is very important, reflecting contamination by initial ^{230}Th (San Miguel et al. 2001). ^{230}Th and ^{232}Th are two long-life radioisotopes of Th element and for that during any chemical process that have to be the same behavior. Therefore, during the chemical process of phosphoric acid production, the ^{230}Th/^{232}Th activity ratio measured in the raw material has to be the same that in the final products (PG and phosphoric acid), the radionuclide concentrations in the sulfuric acid are negligible. In other words, activity ratios of two radionuclides belonging to the same element (U, Th, Ra) can be used as markers of the processes involved in specific transformation. For that, it is interesting to calculate these activity ratios in the different materials obtained from specific raw materials. During the acidification of phosphate

rocks, 80% of ^{230}Th fractionates into PG, and this has been attributed to a number of factors including redox potential, digestion temperature during rock processing, sorption of humic substances and clays, and co-precipitation with fluorides (Mazzilli et al. 2000). ^{232}Th is very minor presence in phosphate minerals (Akyüz et al. 2000), and ^{230}Th/^{232}Th ratio in Moroccan phosphate rock (sedimentary origin) is approximately 80 (Guerrero et al. 2020). This ratio was slightly weakened in the PG which is 67 ± 10 (Table 3).

The ^{234}U/^{238}U ratios are close to the standard value of 1 for soils (Minteer et al. 2007), meaning that a centuries-old balance between ^{238} and ^{234}U is found in all raw materials.

Table 3 shows a potential absence of secular equilibrium between ^{232}Th and ^{226}Ra and for lime and between ^{234}U and ^{230}Th for lime and PG, respectively. Likewise, the effective specific activity of natural radionuclides of L ($A_{eff} = 0.09*A_K + A_{Ra} + 1.3*A_{Th}$) changes during the heat treatment, and the fuel, used for calcination, contributes significantly to the increase in the activity of ^{226}Ra in L (Mikhnev et al. 2019).

The concentrations of the gamma emitters of the raw materials solids are given in Table 3. The concentration of ^{226}Ra (via ^{214}Pb, 351.9 keV) for B and L is 24.7 ± 1.3 Bq kg^{-1} and 11.1 ± 0.9 Bq kg^{-1}, respectively. For PG, the concentration of ^{226}Ra is equal to 815 ± 33 Bq kg^{-1}. PG shows a relative enrichment in ^{226}Ra, as observed in previous studies (Azouazi et al. 2001; Becker 1989; Horton et al. 1988). This concentration is higher than that determined for PG of Morocco, which is about 573 Bq kg^{-1} (Qamouche et al. 2020).

For ^{228}Ra (via ^{228}Ac, 911 keV), the activity concentrations were 219 ± 10 Bq kg^{-1}, 6.8 ± 1.7 Bq kg^{-1}, and 14 ± 3 Bq kg^{-1} for B, L, and PG, respectively. In the case of ^{228}Th (via ^{212}Pb, 238 keV), the obtained concentrations were 218 ± 9 Bq kg^{-1}, 8.8 ± 0.6 Bq kg^{-1}, and 13.4 ± 1.0 Bq kg^{-1} for the three samples, respectively.

The ^{40}K (1460.8 keV) concentrations in B, L, and PG are respectively 285.1 ± 14 Bq kg^{-1}, 87.7 ± 9 Bq kg^{-1}, and 29.5 ± 12 Bq kg^{-1} lower than the overall average soil value 400 ± 24 Bq kg^{-1} (UNSCEAR 2008). B appears to be rich in ^{40} K, probably due to the presence of the K-feldspars (Fig. S1A in supplementary materials). X-ray fluorescence showed the presence of 4.67% K in B (Table S2 in supplementary materials).

Mortars characterization

XRD analysis after 28 days of hydration for PG0 and PG8 shows the formation of calcium silicate hydrate (CSH) and hemicarbonaluminate (Hc) by adding 8% of L to B and ettringite with the addition of 8% of PG to B-L mixture (Fig. 3S in supplementary materials). The formation of CSH is important in our study because these gels improve the compressive strength of bentonite-lime mixture and also when we added the PG. These gels form just after 3 days of hydration and may be before this time, thanks to the pozzolanic reaction. SEM image of PG8 showed needle-shaped crystals of ettringite (Fig. 4S in supplementary materials). The formation of the ettringite increases the mechanical performance of the material (Oumnih et al. 2019).

According to Fig. 4SC in supplementary materials, the best compressive strength for PG0–PG32 (Table 1) was observed for the PG8 mixture with a value of 1.54 MP.

Leachate analysis

Leachates of raw material and mortar specimens

Figure 3 shows the transfer factors (TF) of chemical elements from solid matter to leachate. In the case of B, the chemical elements with the highest transfer factors are Cs (13.16%), Ta (10.01%), and As (4.70%). The elements with the highest transfer factors are (Ba (9.21%), Rb (8.42%), and Li (5.40%)) for lime and (Rb (12.52%), Cd (9.67%), Zn (9.29%), and Ni (8.13%)) for PG. TFs for (As, Cd, Pb, Cu, Cr, Ni, Zn, Mn) were found to be highest for PG manufactured in Huelva (Spain) (Pérez-Moreno et al. 2023).

Tables 4 and 5 show the concentration of some PTEs (As, Cd, Cr, Cu, Ni, Pb, Mn, and Zn) released by the raw materials B, L, and PG in demineralized water and of the leachates of the mortars PG0, PG8L0, PG2, PG8, PG16, and PG32 after 24 h of leaching. The release of PTEs from L is very low compared with B and PG. According to the Table 4, the most PTEs released by B are As (4.70%), Cu (3.65), Zn (1.84%), Cr (1.33) and Ni (0.88). The release of PTEs from L is very low compared with B and PG. In addition, PG as industrial wastes release high amount of PTEs: Cd (9.67%), Zn (9.28%), Ni (8.13%), Cu (4.06%), Mn (2.63%), Pb (1.01%), and As (0.83%). The mobility of PTEs is more important in the case of PG. Comparing our results in the case of the leaching of PG with other work, we can conclude that the most PTEs mobility are observed for As, Cd, Cr, Ni, Cu, Pb, and Zn. The study by Rafael Pérez-López et al. (2007) on the Huelva PG (Spain) found mobility rates of 6%, 5%, 5%, and 2%, respectively, for Cu, Cd, Ni, and Zn. The leaching results of PG, originating from Aqaba and Eshidiya in Jordan, showed that approximately 3% As, 1% Cd, 5% Cr, 9% Cu, and 3% Zn are transferred to the surrounding aquatic environment and/or soils (Al-Hwaiti et al. 2010).

When B is mixed with hydraulic L (sample PG0, Table 5), the amount of arsenic released becomes very low (0.0332 mg kg^{-1}), which may be due to its stabilization by the CSH cement gel produced by the reaction of B with L (Fig. 3S). In the leachate of the sample containing only PG and B (without the addition of L, PG8L0 specimen), arsenic is detected. Therefore, the As concentration becomes undetectable only

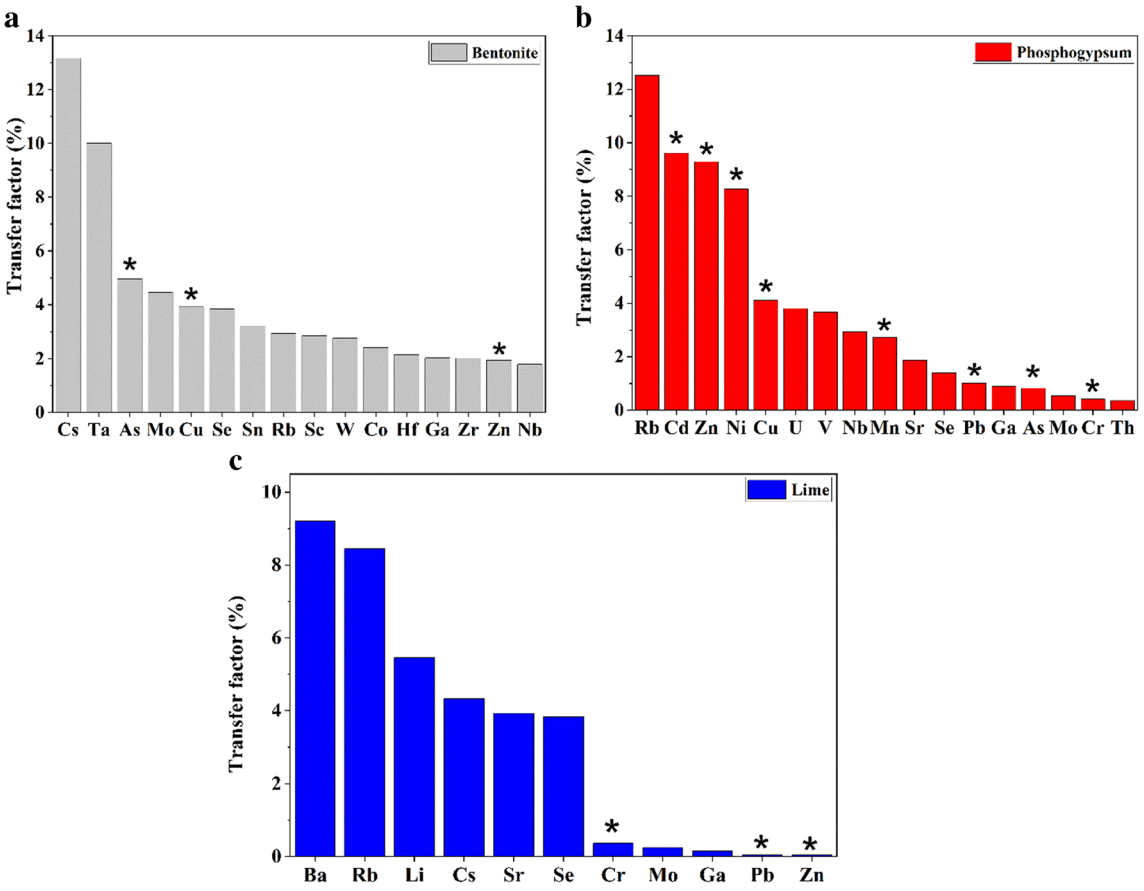

Fig. 3 Transfer factors for **A** bentonite, **B** PG, and **C** lime. *Represents PTEs (As, Cd, Pb, Cu, Cr, Ni, Zn, Mn)

Table 4 Concentrations and transfer factor of PTEs in leachates of raw materials

Elements (mg kg^{-1})	As	Cd	Cr	Cu	Ni	Pb	Mn	Zn
B	0.41	< DL	0.13	0.18	0.02	0.09	1.28	5.17
L	< DL	< DL	0.12	< DL	< DL	0.04	< DL	0.04
PG	0.03	0.31	0.15	0.22	0.31	0.05	0.34	1.14
	TF							
B	4.70	-	1.33	3.65	0.88	0.55	0.9	1.84
L	-	-	0.36	-	-	0.04	-	0.04
PG	0.83	9.67	0.41	4.06	8.13	1.01	2.63	9.28

DL detection limit

Table 5 Concentrations of PTEs in leachates of mortar specimens

Elements (mg kg^{-1})	As	Cd	Cr	Cu	Ni	Pb	Mn	Zn	Sb
PG0	0.0332	< DL	0.0566	0.0204	< DL	< DL	< DL	0.0218	< DL
PG8L0	0.0561	< DL	< DL	0.0057	0.0054	< DL	0.0589	0.822	< DL
PG2	0.00513	< DL	0.0425	< DL	< DL	< DL	< DL	< DL	< DL
PG8	< DL	< DL	0.0709	< DL	< DL	< DL	< DL	< DL	< DL
PG16	< DL	< DL	0.0779	< DL	< DL	< DL	< DL	0.0182	< DL
PG32	< DL	< DL	0.0647	0.0053	< DL	< DL	< DL	0.0235	< DL

DL detection limit

when L is added to B. This can be interpreted by the formation of the cemented gel CSH through pozzolanic reactions between L and B, which consolidates B grains and consequently prevents the release of arsenic. In leachate from specimen containing PG and B, cadmium, along with most potentially toxic trace elements, have concentrations below the detection limit of ICP-MS. This was also confirmed for the sample containing 32% of PG. This result implies that the B-L-PG mixture has the capability to trap PTEs, especially those which high transfer factors, such as Cd and As.

Kinetic study of leaching

Physicochemical parameters Figure 4 shows the temporal evolution of pH, EC, and redox potential in the leachates of specimens PG0, PG8L0, PG2, PG8, PG32. The pH of leachates from samples containing L increases considerably during the first 3 days followed by a gradual stabilization. The pH of the leachates increases from 7.3 to values exceeding 12 (Fig. 4A). PG is rich in residual acidity, reflected in its leachate with a pH of 2.67. However, the addition of PG to B (PG8L0 specimen) does not influence the pH of the leachates. This is probably due to the neutralization of the acidity of PG by particle–particle cementation during the aging of the clay specimen. Indeed, the setting and the hardening of the clay specimen mixed with water result from particle rearrangements and particle–particle cementation (Dexter et al. 1988). For B-L-PG mixtures (PG2–PG32), the pH of the leachate at equilibrium decreases with an increasing quantity of added PG.

The EC (Fig. 4B) of the leachates from the various hardened specimens is very low compared to that of leachates from powdered raw materials. In raw earth specimens, the particles are coated in a cemented matrix, impeding the diffusion of water towards the core of the specimens. This makes difficult the contact between non-hydrated solid particles and water, reducing the release of ions into the water and, consequently, EC. The EC curves show a relaxation period of 2 to 3 days, corresponding to the diffusion of water molecules, the development of microcracks, and the dissociation of crystalline structures under the action of electrostatic forces in the solid. After 5 days of leaching, a strong increase in EC is observed, corresponding to the stage of ions release, hydration, and dispersion of ions in the solution. After about 10 days of leaching, the equilibrium is established, and EC stabilizes. The increase in electrical conductivity could be

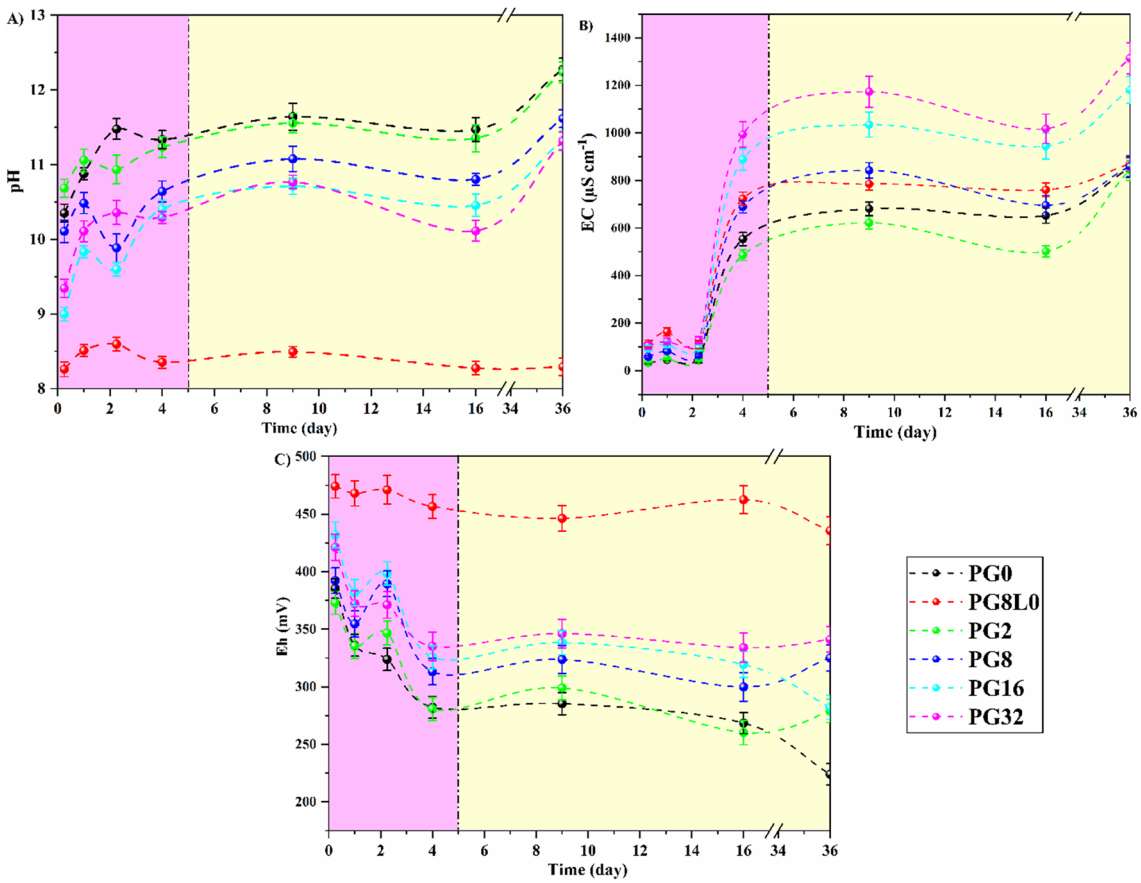

Fig. 4 Evolution of physicochemical parameters. **A** pH. **B** EC (µS/cm). **C** Eh (mV) of leachates

due to the release of Ca^{2+}, OH^- from the L and H^+, and SO_4^{2-} from the PG. Indeed, the molar conductivities per unit charge concentration $\Lambda°$ are significant, equal to 11.9, 19.8, 16, and 34.9 m^2 S mol^{-1}, respectively, for Ca^{2+}, OH^-, SO_4^{2-}, and H^+ (Vanysek 1993).

The redox potential of the PG8L0 leachate remains constant at around 450 mV throughout the leaching period. The dissolved ions have a strong tendency to be reduced and to receive electrons from other chemical species in the solution (Fig. 4C). When L is added to the specimens (PG0–PG32), the initial redox potential of the leachates is 400 mV, and it undergoes a decrease during the first 5 days, followed by stabilization. This decrease in the redox potential is probably due to the oxidation of the dissolved reducing species and the formation of hydroxides facilitated by OH^- supplied by L. The pH, EC, and redox potential curves show stable levels after 10 days of leaching.

Cation release The concentration of cations in the leachate of PG0, PG8, and PG32 mixtures is represented in Fig. 5. Between 0.25 and 5 days of leaching, the release of the cations is rapid and significant. After 15 days, the release is slowed down and subsequently stabilizes. For the three specimens, Sr^{2+} is the most released cation, with concentration after 36 days of leaching of 0.041, 0.091, and 0.185 mg kg^{-1} for PG0, PG8, and PG32, respectively. In the leachate of powdered raw materials, especially L and PG, Sr^{2+} stands out among the predominant cations. In the case of the specimen containing 92% B and 8% L (PG0), the second-ranking released cation, after Sr, is Cr. This element, present in traces in B and PG, does not appear in the leachates of raw material.

For PG8, with the exception of Ba, Sr, and V showing increases, the concentrations of other cations in the leachates remain unchanged. With a significant quantity of PG (32% in the case of PG32), an increase is observed in the concentrations of Ba, Sr, V and Zn. The concentration of Cs increases in the leachates of PG8 and PG32, suggesting its release from B. Although Cd is one of the most leached elements from PG (Fig. 3), it does not appear in the leachate of samples containing PG. Montmorillonite has a strong ability to adsorb Cd ions by a precipitation process to form hydroxide at pH between 6 and 9. Adsorption is more favored with

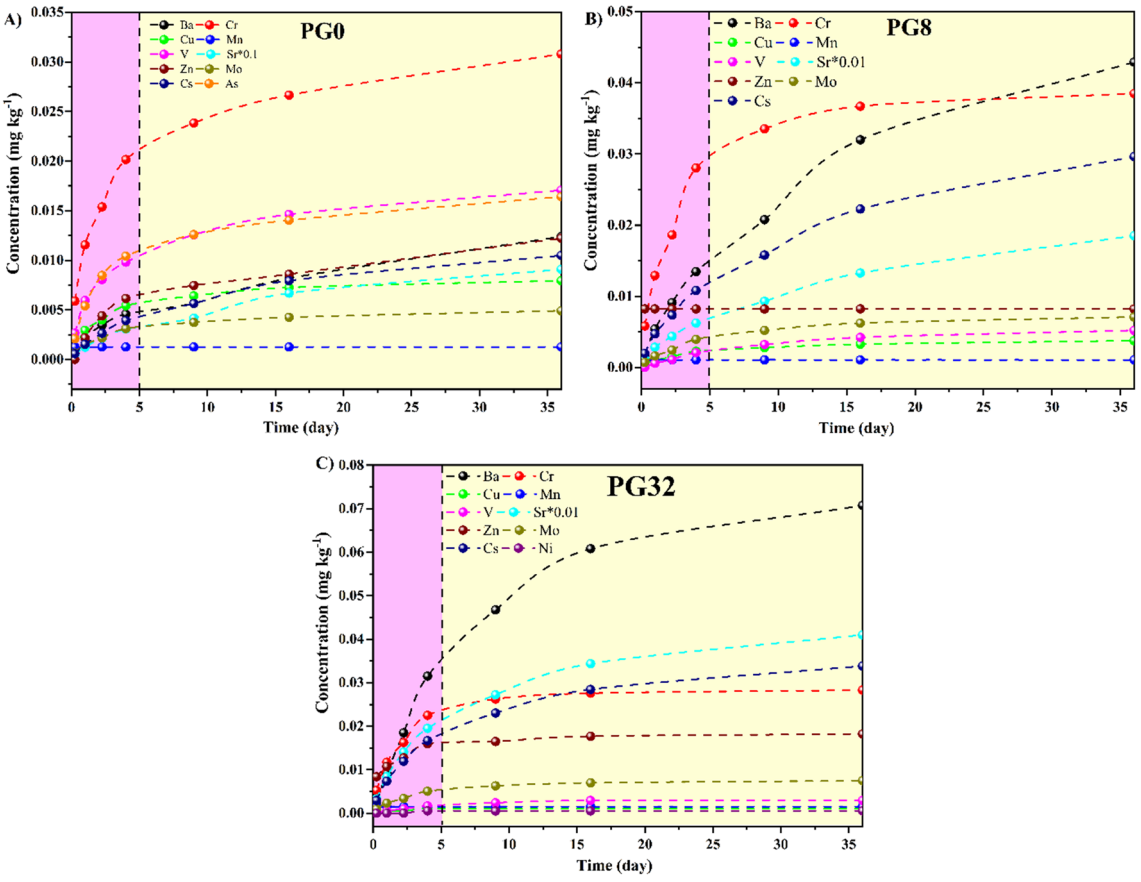

Fig. 5 Cations release from mortars to distilled water with time (note: Sr concentration was divided by 10 for PG0 and by 100 for PG8 and PG32)

increased contact time between Cd and montmorillonite particles (Altin et al. 1999; Ayouch et al. 2020).

The PG0 specimen releases a very small amount of arsenic; however, with the addition of PG, this element does not appear. The release of cations in water by B-L-PG raw earth mortars, although very insignificant, stabilizes from the first 15 days, demonstrating the stability of the material.

Anion release Figure 6 shows the evolution of the release of anions (Cl^-, SO_4^{2-}, F^-, NO_3^-) in demineralized water. The release kinetics are important during the first days and decelerate after 15 days of leaching. Chloride ions may originate from clay, as montmorillonite and kaolinite, especially when montmorillonite and kaolinite are out of brine, and they grow in the interlayer space, initially filled by oversaturated brine. This process involves crystal nucleation and the growth of NaCl (Dashtian et al. 2017). The addition of PG causes the release of sulfates into the water, apparently without disrupting the release of chloride ions by the B-L matrix. Even with a high dose of PG (specimen PG32), the concentration of fluoride ions in the leachate does not increase and remains negligible, despite PG normally containing 0.6 to 1.8 mg kg^{-1} of F^- (Ennaciri et al. 2020). This is probably due to the conversion, by L, of ions to insoluble calcium fluoride (CaF_2) whose solubility constant is low ($Ksp = 3.9\ 10^{-11}$) (Lokshin and Tareeva 2015). The analysis did not show the presence of PO_4^{3-} ions in the leachates of the samples containing PG, probably due to the formation of insoluble hydrated calcium phosphates (e.g., brushite, hydroxyapatite).

Radionuclides release

Alpha emitters for raw materials leachates Table 6 gives the concentrations of alpha emitters ($^{238,234}U$, $^{232,230}Th$, and ^{210}Po) in the solutions, filtered after 24-h leaching period of raw materials (B, L, and PG). The highest concentration of global-alpha activity is found in PG, followed by B and by far by L. The release of radionuclides is seemingly independent of their content in the raw materials but rather influenced by on the nature of the nuclide and its mobility. Calculation of the TFs of the radionuclides analyzed in the raw materials shows high mobility alpha-emitting radionuclides in water from bentonite. This mobility is relatively lower in the case of PG and lime. Despite a higher content of ^{230}Th (782.4 ± 53.9 Bq kg^{-1}) compared to ^{210}Po (699 ± 3 Bq

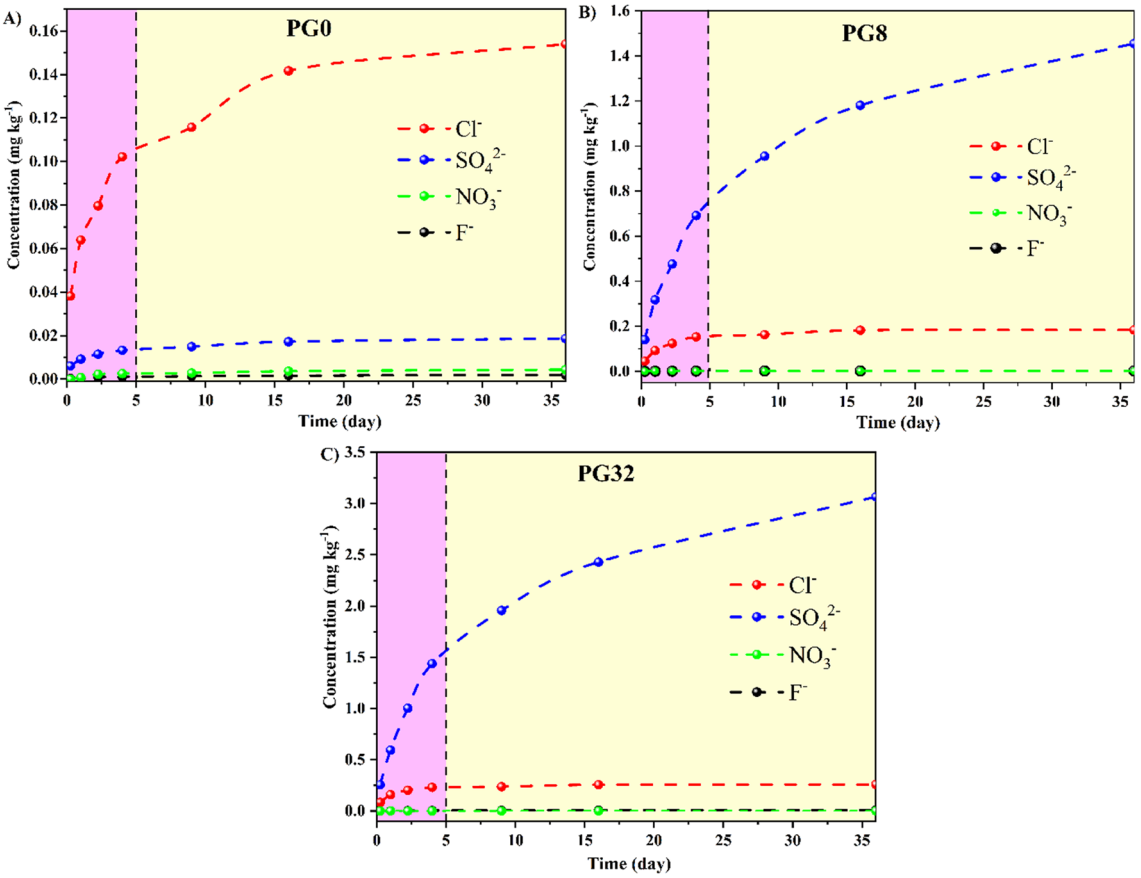

Fig. 6 Anions release from mortars to distilled water with time

Table 6 Concentrations and transfer factor of alpha particle emitting radionuclides in raw material leachates (leaching time = 24 h)

Samples	^{210}Po	^{234}U	^{238}U	^{232}Th	^{230}Th	Global-alpha activities	^{230}Th/^{232}Th
Bq kg^{-1}							
Leachate of B	1 ± 0.05	< DL	< DL	0.74 ± 1.10	4.40 ± 1.10	6.3	6.03
Leachate of L	0.023 ± 0.004	< DL	< DL	0.31 ± 0.02	0.72 ± 0.03	1.1	2.33
Leachate of PG	3.4 ± 0.3	1.6 ± 0.08	< DL	0.49 ± 0.02	1.8 ± 0.1	7.3	3.67
TF (%)							
B	5.43	-	-	10.26	70.85	-	-
L	0.32	-	-	0.17	2.62	-	-
PG	0.49	2.11	-	4.26	0.02	-	-

DL detection limit

kg^{-1}) in PG (Table 3), the TF of ^{230}Th (0.02%) is negligible compared to that of ^{210}Po (0.49%) (Table 6).

Alpha emitters for PG32 leachates Mortars containing 32% PG were chosen for the alpha emission radionuclide release study. The temporal evolution of the concentrations of the alpha-emitting radionuclides (^{238,234}U, ^{232,230}Th, and ^{210}Po) in the leachate of PG32 specimen shows saturation after 4 days of leaching (Fig. 7A). Among the radionuclides, ^{210}Po shows the highest release into the leachate from PG32. However, the quantity of each radionuclide released is very small compared with the quantity released from raw materials. Similarly, the overall alpha activities in the leachate of the PG32 samples are very low compared with the overall alpha activities in the leachate of the raw materials (Fig. 7B).

Based on the mass composition of the PG32 sample, containing 60% B, 8% L, and 32% PG, and the alpha activities in the solid raw materials ($A_{exp(S)}$) (Table 3) and in their respective leachates ($A_{exp(L)}$) (Table 6), we calculate the optimum concentrations $A_{opt(S)}$ from the solid raw materials and $A_{opt(L)}$ from the concentrations of the raw materials in the leachate (Table 7). When materials are compacted into the PG32 mortar sample, radionuclide mobility decreases, and release is greatly reduced. The overall alpha activities recorded (0.0017 Bq kg^{-1}) in the PG32 leachate represent only 0.13% of the overall optimum activity calculated from the activities of the raw material leachates. The formulation of hydrated B-L-PG mixtures makes proves effective in confining the radionuclides present in the raw materials, particularly in the PG.

For the purpose of this research, the optimal mixture for the leaching of B-L-PG was determined to be PG8. This specific proportion was selected based on initial experiments that showed it provided the most effective balance between reactivity and stability. The equal parts of bentonite, lime,

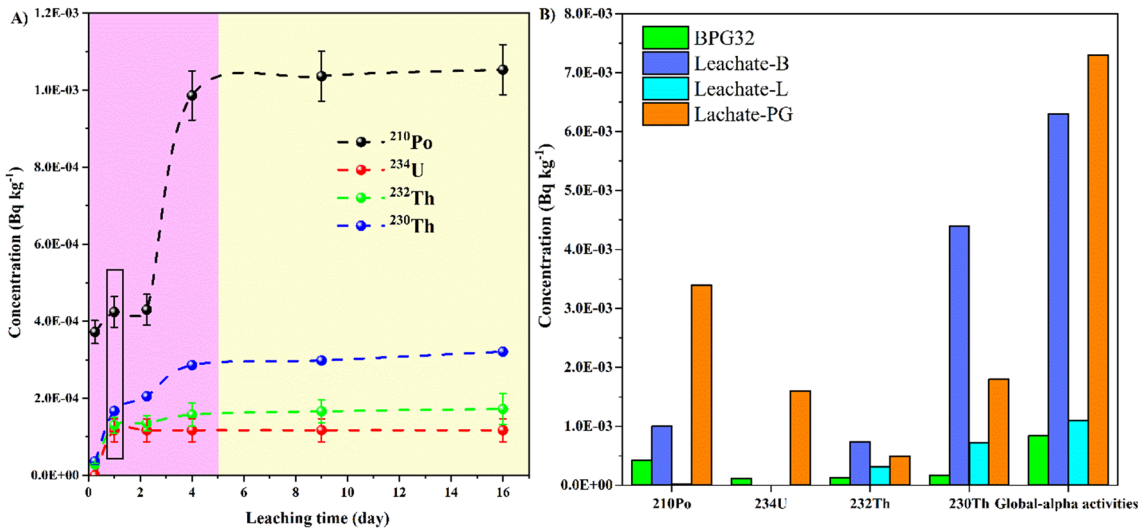

Fig. 7 **A** Concentrations of alpha-emitting radionuclides of PG32 leachates varying the leaching time. **B** Concentrations of alpha-emitting radionuclides of PG32, B, L, and PG leachates after 1 day

Table 7 Release rate of radionuclides into water after a leaching period of 16 days for the PG32 specimen

	^{210}Po	^{234}U	^{232}Th	^{230}Th
Bq kg^{-1}				
A_{exp}	0.0011	0.0001	0.0002	0.0003
$A_{opt(L)}$	1.68984	0.512	0.6256	3.2736
R_L (%)	0.07	0.02	0.03	0.01
$A_{opt(S)}$	235.3	42.4	22.6	256.3
R_S (%)	4.67E-04	2.36E-04	8.85E-04	1.17E-04

and PG ensure a consistent and uniform blend, promoting efficient interaction among the components. This ratio maximizes the leaching efficiency by enhancing the pozzolanic reaction, which helps in immobilizing contaminants and improving the overall material properties.

Conclusion

This study was focused on the hypothesis that pollutants can be immobilized by phosphogypsum (PG) in raw clayey soils through the incorporation of B and hydraulic L. PG was mixed with B and L at levels ranging from 0%, 2%, 8%, 16%, and 32% by weight of dry soil, with a fixed L content of 8%. The properties of raw materials, and hardened specimens, were studied. This included physicochemical, radioactivity and geotechnical characterizations of solids, leaching tests, and chemical and radioactivity analyses of leachates. The key findings can be summarized as follows:

(1) PG contains high concentrations of trace elements (Cd, U, and Y) exceeding the recommended composition of the upper continental crust. In addition, it contains high concentrations of U series radionuclides (^{226}Ra, ^{210}Po, and ^{230}Th).
(2) Cd, Zn, and Ni are the PTEs having the highest transfer factors from PG to water.
(3) PG leachates contain concentrations of emitting radionuclides 210Po, 234U, 232Th, and 230Th of 3.4 ± 0.3 Bq kg^{-1}, 1.6 ± 0.08 Bq kg^{-1}, 0.49 ± 0.02 Bq kg^{-1}, and 1.8 ± 0.1 Bq kg^{-1}, respectively.
(4) Monitoring of physicochemical parameters, cations and anions concentrations, and the activity of alpha-emitting radionuclides in hardened raw earth mortars containing PG-B-L for 36 days showed that the exchange with water, generally, stops after 10 days of leaching. This result seems interesting and original, but it needs to be confirmed by long-term tests carried out on open-air PG deposits.
(5) When PG is mixed with B or B-L, cadmium and several PTEs do not appear in the leachates.
(6) The quantity of alpha-emitting radionuclides (^{238,234}U, ^{232,230}Th, and ^{210}Po) released by the PG-B-L specimen is very small compared to those released by the raw materials.
(7) Hydration of the B-L mixture leads to the formation of cemented gel (CSH) and hemicarbonaluminate (Hc). The addition of PG to the B-L mixture forms needle-like ettringite crystals.
(8) The greatest mechanical compressive strength is 1.54 MPa found when the quantity of 8% PG is added to the B-L mixture.

Supplementary Information The online version contains supplementary material available at https://doi.org/10.1007/s11356-024-34694-9.

Author contribution Harrou Achraf "a" — conceptualization, data curation, formal analysis, investigation, methodology, validation, writing — original draft, and writing — review and editing. Meriam El Ouahabi "b" — conceptualization, data curation, formal analysis, investigation, methodology, validation, writing — original draft, and writing — review and editing. Nathalie Fagel "b" — conceptualization, data curation, formal analysis, investigation, methodology, validation, writing — original draft, and writing — review and editing. Alejandro Barba-Lobo "c" — conceptualization, data curation, formal analysis, investigation, methodology, validation, writing — original draft, writing — review and editing. Silvia M. Pérez-Moreno "c" — conceptualization, data curation, formal analysis, investigation, methodology, validation, writing — original draft, and writing — review and editing. Juan Pedro Bolívar Raya "c" — conceptualization, data curation, formal analysis, investigation, methodology, validation, writing — original draft, and writing — review and editing. ElKhadir Gharibi "a" — conceptualization, data curation, formal analysis, investigation, methodology, validation, writing — original draft, and writing — review and editing.

Data availability The datasets generated and/or analyzed during the current study are available from the corresponding author, upon reasonable request.

Declarations

Ethical approval Not applicable.

Consent to participate Not applicable.

Consent for publication The authors affirm that the work is original, has not been published elsewhere, and is not currently under consideration by another publisher.

Conflict of interest The authors declare no competing interests.

References

Ait Hmeid H, Akodad M, Baghour M, Moumen A, Skalli A, Azizi G, Gueddari H, Maach M, Aalaoul M, Anjjar A, Daoudi L (2021) Valorization of Moroccan bentonite deposits:"purification and treatment of margin by the adsorption process." Molecules 26(18):5528. https://doi.org/10.3390/molecules26185528

Akyüz T, Akyüz S, Varinlioglu A, Kose A (2000) Radioactivity of phosphate ores from Karatas-Mazidag phosphate deposit of Turkey. J Radioanal Nucl Chem Art 243:715–718. https://doi.org/10.1023/A:1010678521556

Al Khaledi N, Taha M, Hussein A, Hussein E, El Yahyaoui A, Haneklaus N (2019) Direct leaching of rare earth elements and uranium from phosphate rocks. IOP Conf Ser: Mater Sci Eng 479(1):012065. https://doi.org/10.1088/1757-899X/479/1/012065

Al-Hwaiti MS, Ranville JF, Ross PE (2010) Bioavailability and mobility of trace metals in phosphogypsum from Aqaba and Eshidiya. Jordan Geochem 70(3):283–291. https://doi.org/10.1016/j.chemer.2010.03.001

Altin O, Ozbelge OH, Dogu T (1999) Effect of pH, flow rate and concentration on the sorption of Pb and Cd on montmorillonite: I Experimental. J Chem Technol Biotechnol 74(12):1131–1138. https://doi.org/10.1002/(SICI)1097-4660(199912)74:12<1131::AID-JCTB158>3.0.CO;2-0

Ayouch I, Barrak I, Kassab Z, El Achaby M, Barhoun A, Draoui K (2020) Improved recovery of cadmium from aqueous medium by alginate composite beads filled by bentonite and phosphate washing sludge. Colloids Surf A 604:125305. https://doi.org/10.1016/j.colsurfa.2020.125305

Azouazi M, Ouahidi Y, Fakhi S, Andres Y, Abbe JC, Benmansour M (2001) Natural radioactivity in phosphates, phosphogypsum and natural waters in Morocco. J Environ Radioact 54(2):231–242. https://doi.org/10.1016/S0265-931X(00)00153-3

Barba-Lobo A, San Miguel EG, Lozano RL, Bolívar JP (2021) A general methodology to determine natural radionuclides by well-type HPGe detectors. Measurement 181:109561. https://doi.org/10.1016/j.measurement.2021.109561

Becker P (1989) Phosphates and phosphoric acid: raw materials, technology, and economics of the wet process. Second edition, Marcel Dekker, Inc.

Belahbib L, Arhouni FE, Boukhair A, Essadaoui A, Ouakkas S, Hakkar M, Abdo MA, Benjelloun M, Bitar A, Nourreddine A (2021) Impact of phosphate industry on natural radioactivity in sediment, seawater, and Coastal Marine Fauna of El Jadida Province Morocco. J Hazard Toxic Radioact Waste 25(1):04020064. https://doi.org/10.1061/(ASCE)HZ.2153-5515.0000563

Bhawan P, Nagar EA (2014) Guidelines for management, handling, utilization and disposal of phosphogypsum generated from phosphoric acid plants. Central Pollution Control Board, New Delhi.

Bodin S, Fröhlich S, Boutib L, Lahsini S, Redfern J (2011) Early Toarcian source-rock potential in the central High Atlas basin (Central Morocco): regional distribution and depositional model. J Pet Geol 34(4):345–363. https://doi.org/10.1111/j.1747-5457.2011.00509.x

Bolıvar JP, Garcıa-Tenorio R, Mas JL, Vaca F (2002) Radioactive impact in sediments from an estuarine system affected by industrial wastes releases. Environ Int 27(8):639–645. https://doi.org/10.1016/S0160-4120(01)00123-4

Cánovas CR, Chapron S, Arrachart G, Pellet-Rostaing S (2019) Leaching of rare earth elements (REEs) and impurities from phosphogypsum: a preliminary insight for further recovery of critical raw materials. J Clean Prod 219:225–235. https://doi.org/10.1016/j.jclepro.2019.02.104

Dashtian H, Wang H, Sahimi M (2017) Nucleation of salt crystals in clay minerals: molecular dynamics simulation. J Phys Chem Lett 8(14):3166–3172. https://doi.org/10.1021/acs.jpclett.7b01306

Ddani M, Meunier A, Zahraoui M, Beaufort D, El Wartiti M, Fontaine C, Boukili B, El Mahi B (2005) Clay mineralogy and chemical composition of bentonites from the Gourougou volcanic massif (northeast Morocco). Clays Clay Miner 53(3):250–267. https://doi.org/10.1346/CCMN.2005.0530305

Dexter AR, Horn R, Kemper WD (1988) Two mechanisms for age-hardening of soil. J Soil Sci 39(2):163–175. https://doi.org/10.1111/j.1365-2389.1988.tb01203.x

Dubchak S (2018). Distribution of strontium in soil: interception, weathering, speciation, and translocation to plants. (eds) Behaviour of Strontium in Plants and the Environment. Springer, Cham. https://doi.org/10.1007/978-3-319-66574-0_3

Dueñas C, Liger E, Cañete S, Pérez M, Bolívar JP (2007) Exhalation of 222Rn from phosphogypsum piles located at the southwest of Spain. J Environ Radioact 95(2–3):63–74. https://doi.org/10.1016/j.jenvrad.2007.01.012

Dueñas C, Fernández MC, Cañete S, Pérez M (2010) Radiological impacts of natural radioactivity from phosphogypsum piles in Huelva (Spain). Radiat Meas 45(2):242–246. https://doi.org/10.1016/j.radmeas.2010.01.007

El Zrelli R, Rabaoui L, Daghbouj N, Abda H, Castet S, Josse C, van Beek P, Souhaut M, Michel S, Bejaoui N, Courjault-Radé P (2018) Characterization of phosphate rock and phosphogypsum from Gabes phosphate fertilizer factories (SE Tunisia): high mining potential and implications for environmental protection. Environ Sci Pollut Res Int 25:14690–14702. https://doi.org/10.1007/s11356-018-1648-4

El Zrelli R, Rabaoui L, van Beek P, Castet S, Souhaut M, Grégoire M, Courjault-Radé P (2019) Natural radioactivity and radiation hazard assessment of industrial wastes from the coastal phosphate treatment plants of Gabes (Tunisia, southern Mediterranean Sea). Mar Pollut Bull 146:454–461. https://doi.org/10.1016/j.marpolbul.2019.06.075

Ennaciri Y, Zdah I, El Alaoui-Belghiti H, Bettach M (2020) Characterization and purification of waste phosphogypsum to make it suitable for use in the plaster and the cement industry. Chem Eng Commun 207(3):382–392. https://doi.org/10.1080/00986445.2019.1599865

Ermakov V, Bech J, Gulyaeva U, Tyutikov S, Safonov V, Danilova V, Roca N (2020) Relationship of the mobile forms of calcium and strontium in soils with their accumulation in meadow plants in the area of Kashin-Beck endemia. Environ Geochem Health 42:159–171. https://doi.org/10.1007/s10653-019-00323-5

Gaona X, Kulik DA, Macé N, Wieland E (2012) Aqueous–solid solution thermodynamic model of U (VI) uptake in C-S–H phases. Appl Geochem 27(1):81–95. https://doi.org/10.1016/j.apgeochem.2011.09.005

Guerrero JL, Gutiérrez-Álvarez I, Mosqueda F, Olías M, García-Tenorio R, Bolívar JP (2019) Pollution evaluation on the saltmarshes under the phosphogypsum stacks of Huelva due to deep leachates. Chemosphere 230:219–229. https://doi.org/10.1016/j.chemosphere.2019.04.212

Guerrero JL, Pérez-Moreno SM, Mosqueda F, Gázquez MJ, Bolívar JP (2020) Radiological and physico-chemical characterization of materials from phosphoric acid production plant to assess the workers radiological risks. Chemosphere 253:126682. https://doi.org/10.1016/j.chemosphere.2020.126682

Guido-Garcia F, Sakamoto F, David K, Kozai N, Grambow B (2021) Radiocesium in Shiitake mushroom: accumulation in living fruit bodies and leaching from dead fruit bodies. Chemosphere 279:130511. https://doi.org/10.1016/j.chemosphere.2021.130511

Han B, Weatherley AJ, Mumford K, Bolan N, He JZ, Stevens GW, Chen D (2022) Modification of naturally abundant resources for remediation of potentially toxic elements: a review. J Hazard Mater 421:126755. https://doi.org/10.1016/j.jhazmat.2021.126755

Harrou A, Gharibi EK, Taha Y, Fagel N, El Ouahabi M (2020) Phosphogypsum and black steel slag as additives for ecological bentonite-based materials: microstructure and characterization. Minerals 10(12):1067. https://doi.org/10.3390/min10121067

Hilton J (2008) Towards a management and regulatory strategy for phosphoric acid and phosphogypsum as co-products. In Naturally Occurring Radioactive Material (NORM V) (Proc. Int. Symp. Seville, 2007), IAEA, Vienna (pp. 281–295).

Horton TR, Blanchard RL, Windham ST (1988) A long-term study of radon and airborne particulates at phosphogypsum stacks in

Central Florida (no. EPA/520/5–88–021). Environmental Protection Agency, Montgomery, AL (USA). Eastern Environmental Radiation Facility.

IAEA (2013) Radiation protection and management of NORM residues in the phosphate industry. Internat. Atomic Energy Agency. Safety Reports Series, (78).

Kabata-Pendias A (2000) Trace elements in soils and plants. 3rd Edition, CRC press. https://doi.org/10.1201/9781420039900

Kechiched R, Laouar R, Bruguier O, Kocsis L, Salmi-Laouar S, Bosch D, Ameur-Zaimeche O, Foufou A, Larit H (2020) Comprehensive REE+ Y and sensitive redox trace elements of Algerian phosphorites (Tébessa, eastern Algeria): a geochemical study and depositional environments tracking. J Geochem Explor 208:106396. https://doi.org/10.1016/j.gexplo.2019.106396

Kretschmer S (2010) The influence of particle size, composition, and transport on the distribution of 230Thxs, 231Paxs, and 10Be in marine sediments (Doctoral dissertation, Universität Bremen).

Kumar S, Dutta RK, Mohanty B (2014) Engineering properties of bentonite stabilized with lime and phosphogypsum. J Civ Eng Manag 22(4):35–44. https://doi.org/10.2478/sjce-2014-0021

Lamrani O, Aabi A, Boushaba A, Seghir MT, Adiri Z, Samaoui S (2021) Bentonite clay minerals mapping using ASTER and field mineralogical data: a case study from the eastern Rif belt. Morocco Remote Sens Appl Soc Environ 24:100640. https://doi.org/10.1016/j.rsase.2021.100640

Lokshin EP, Tareeva OA (2015) Production of high-quality gypsum raw materials from phosphogypsum. Russ J Appl Chem 88:567–573. https://doi.org/10.1134/S1070427215040023

Ludwig KA, Shen CC, Kelley DS, Cheng H, Edwards RL (2011) U-Th systematics and 230Th ages of carbonate chimneys at the Lost City Hydrothermal Field. Geochim Cosmochim Acta 75(7):1869–1888. https://doi.org/10.1016/j.gca.2011.01.008

Mashifana T, Okonta FN, Ntuli F (2018) Geotechnical properties and application of lime modified phosphogypsum waste. Mater Sci 24(3):312–318. https://doi.org/10.5755/j01.ms.24.3.18232

Mazzilli B, Palmiro V, Saueia C, Nisti MB (2000) Radiochemical characterization of Brazilian phosphogypsum. J Environ Radioact 49(1):113–122. https://doi.org/10.1016/S0265-931X(99)00097-1

Mikhnev IP, Salnikova NA, Mikhneva SV (2019) Effect of thermal treatment of building materials on natural radionuclides effective specific activity. In Mater Sci Forum 945:30–35. https://doi.org/10.4028/www.scientific.net/MSF.945.30

Minteer M, Winkler P, Wyatt B, Moreland S, Johnson J, Winters T (2007) Reliability of using 238U/235U and 234U/238U ratios from alpha spectrometry as qualitative indicators of enriched uranium contamination. Health Phys 92(5):488–495. https://doi.org/10.1097/01.HP.0000254847.21026.7c

Moreno SP, Romero C, Guerrero JL, Barba-Lobo A, Gázquez M, Bolívar JP (2023) Evolution of the waste generated along the cleaning process of phosphogypsum leachates. J Environ Chem Eng 11(6):111485. https://doi.org/10.1016/j.jece.2023.111485

Mosai AK, Chimuka L, Cukrowska EM, Kotzé IA, Tutu H (2019) The recovery of rare earth elements (REEs) from aqueous solutions using natural zeolite and bentonite. Water Air Soil Pollut 230:1–17. https://doi.org/10.1007/s11270-019-4236-4

Mukaba JL, Eze CP, Pereao O, Petrik LF (2021) Rare earths' recovery from phosphogypsum: an overview on direct and indirect leaching techniques. Minerals 11(10):1051. https://doi.org/10.3390/min11101051

Nordstrom DK, Wilde FD (1998) Reduction-oxidation potential (electrode method), in: National Field Manual for the Collection of Water Quality Data, U.S. Geological Survey Techniques of Water-Resources Investigations, Book 9, chapter 6.5.

Oumnih S, Bekkouch N, Gharibi EK, Fagel N, Elhamouti K, El Ouahabi M (2019) Phosphogypsum waste as additives to lime stabilization of bentonite. Sustain Environ Res 29(1):1–10. https://doi.org/10.1186/s42834-019-0038-z

Papaslioti EM, Pérez-López R, Parviainen A, Phan VT, Marchesi C, Fernandez-Martinez A, Garrido CJ, Nieto JM, Charlet L (2020) Effects of redox oscillations on the phosphogypsum waste in an estuarine salt-marsh system. Chem 242:125174. https://doi.org/10.1016/j.chemosphere.2019.125174

Pérez-López R, Alvarez-Valero AM, Nieto JM (2007) Changes in mobility of toxic elements during the production of phosphoric acid in the fertilizer industry of Huelva (SW Spain) and environmental impact of phosphogypsum wastes. J Hazard Mater 148(3):745–750. https://doi.org/10.1016/j.jhazmat.2007.06.068

Pérez-López R, Castillo J, Sarmiento AM, Nieto JM (2011) Assessment of phosphogypsum impact on the salt-marshes of the Tinto River (SW Spain): role of natural attenuation processes. Mar Pollut Bull 62(12):2787–2796. https://doi.org/10.1016/j.marpolbul.2011.09.008

Pérez-Moreno SM, Gázquez MJ, Pérez-López R, Vioque I, Bolívar JP (2018) Assessment of natural radionuclides mobility in a phosphogypsum disposal area. Chem 211:775–783. https://doi.org/10.1016/j.chemosphere.2018.07.193

Pérez-Moreno SM, Romero C, Guerrero JL, Gázquez MJ, Bolivar JP (2023) Development of a process for the removal of natural radionuclides and other stable pollutants from acid phosphogypsum stacks leachates. J Environ Chem Eng 11(1):109032. https://doi.org/10.1016/j.jece.2022.109032

Periáñez R, Hierro A, Bolívar JP, Vaca F (2013) The geochemical behavior of natural radionuclides in coastal waters: a modeling study for the Huelva estuary. J Mar Syst 126:82–93. https://doi.org/10.1016/j.jmarsys.2012.08.001

Persson BR, Holm E (2011) Polonium-210 and lead-210 in the terrestrial environment: a historical review. J Environ Radioact 102(5):420–429. https://doi.org/10.1016/j.jenvrad.2011.01.005

Qamouche K, Chetaine A, Elyahyaoui A, Moussaif A, Touzani R, Benkdad A, Amsil H, Laraki K, Marah H (2020) Radiological characterization of phosphate rocks, phosphogypsum, phosphoric acid and phosphate fertilizers in Morocco: an assessment of the radiological hazard impact on the environment. Mater Today: Proc 27(3234):3242. https://doi.org/10.1016/j.matpr.2020.04.703

Ramanayaka S, Vithanage M, Sarmah A, An T, Kim KH, Ok YS (2019) Performance of metal–organic frameworks for the adsorptive removal of potentially toxic elements in a water system: a critical review. RSC Adv 9(59):34359–34376. https://doi.org/10.1039/C9RA06879A

Rudnick RL, Gao S (2010) Composition on the continental crust, in Readings from the Treatise on Geochemistry, Holland, HD, Turekian KK (Eds.). Academic Press. p.131

Rutherford PM, Dudas MJ, Samek RA (1994) Environmental impacts of phosphogypsum. Sci Total Environ 149(1–2):1–38. https://doi.org/10.1016/0048-9697(94)90002-7

Sam AK, Ahamed MMO, El Khangi FA, El Nigumi YO (2000) Uranium and thorium isotopes in some red sea sediments. Radiochim Acta 88(5):307–312. https://doi.org/10.1524/ract.2000.88.5.307

San Miguel EG, Bolívar JP, García-Tenorio R, Martín JE (2001) 230Th/232Th activity ratios as a chronological marker complementing 210Pb dating in an estuarine system affected by industrial releases. Environ Pollut 112(3):361–368. https://doi.org/10.1016/S0269-7491(00)00146-9

Shacklette HT, Boerngen JG (1984) Element concentrations in soils and other surficial materials of the conterminous United States, vol 1270. US Government Printing Office, Washington, DC

Silva LF, Oliveira ML, Crissien TJ, Santosh M, Bolivar J, Shao L, Dotto GL, Gasparotto J, Schindler M (2022) A review on the environmental impact of phosphogypsum and potential health impacts through the release of nanoparticles. Chemosphere 286:131513. https://doi.org/10.1016/j.chemosphere.2021.131513

UNSCEAR (2008) United Nations Scientific Committee on the Effects of Atomic Radiation, 2008. Effects of ionizing radiation. Scientific Annexes E, 203–204.

Vanysek P (1993) Ionic conductivity and diffusion at infinite dilution. CRC hand book of chemistry and physics, pp.5–92.

Vriens B, Skierszkan EK, St-Arnault M, Salzsauler K, Aranda C, Mayer KU, Beckie RD (2019) Mobilization of metal (oid) oxyanions through circumneutral mine waste-rock drainage. ACS Omega 4(6):10205–10215. https://doi.org/10.1021/acsomega.9b01270

Authors and Affiliations

Achraf Harrou[1] · Meriam El Ouahabi[2,3] · Nathalie Fagel[3] · Alejandro Barba-Lobo[4] · Silvia M. Pérez-Moreno[4] · Juan Pedro Bolívar Raya[4] · ElKhadir Gharibi[1]

✉ ElKhadir Gharibi
gharibi_elkhadir@yahoo.fr; e.gharibi@ump.ac.ma

Achraf Harrou
achraf.harrou@student.uliege.be; harrou201@gmail.com

Meriam El Ouahabi
meriam.elouahabi@uliege.be

Nathalie Fagel
nathalie.fagel@uliege.be

Alejandro Barba-Lobo
alejandro.barba@dci.uhu.es

Silvia M. Pérez-Moreno
silvia.perez@dci.uhu.es

Juan Pedro Bolívar Raya
bolivar@uhu.es

[1] Laboratory of Applied Chemistry and Environment, Faculty of Sciences, Mohammed First University, 60000 Oujda, Morocco

[2] UR. Art, Archéologie Et Patrimoine (AAP), Université de Liège, B-4000 Liège, Belgium

[3] Géochimie Et Environnement Sédimentaires (AGEs), Laboratoire Argiles, Département de Géologie, Université de Liège, B-4000 Liège, Belgium

[4] Center On Natural Resources, Health and the Environment (RENSMA), University of Huelva, 21071 Huelva, Spain